Infrared Spectroscopy of Polynucleotides in the Carbonyl Region in H_2O Solution: A·U Systems[†]

H. Todd Miles* and Joe Frazier

ABSTRACT: Strong absorbance of water at 1645 cm^{-1} has previously prevented dependable observation of infrared spectra of H_2O solutions in the carbonyl region. We have obtained reliable spectra in pure water and in alcohol–water mixtures in this region and used them to study A·U polynucleotide interaction. Spectra in pure water were obtained by computer subtraction of solvent from that of solution measured in short path length cells. Mixed solvents, by diluting the water, permit use of longer cells and standard double-beam compensation methods. Poly(adenylic acid) in H_2O solution has a strong NH_2 deformation band at 1659 cm^{-1} coupled to an A ring vibration at 1605 cm^{-1}. Poly(uridylic acid) has a broad band at ~1695 cm^{-1}, predominantly C2 carbonyl stretch, an unresolved C4 carbonyl band (probably near 1660 cm^{-1}), and a ring vibration at ~1636 cm^{-1}. The large changes these spectra undergo when helical structures are formed are discussed and compared with changes observed in D_2O.

Infrared spectra of polynucleotides have been extensively investigated in D_2O solution in the region from 1500 to 1800 cm^{-1} (see, for example, Miles, 1958, 1971; Miles & Frazier, 1964; Howard et al., 1966, 1969a, b, 1971, 1976; Cotter & Gratzer, 1969; Thomas, 1969; Tsuboi, 1969; Morikawa et al., 1973; Ikeda et al., 1970; Hattori et al., 1975, 1976). This is the region of double-bond stretching vibrations (C=O, C=N, C=C) of the carbonyl groups and heterocyclic rings of which the bases are composed. It is these portions of the polynucleotides which are directly involved in base pairing and stacking interactions and which thus undergo the most profound environmental changes when helical complexes are formed. Frequencies and intensities of bands corresponding to vibrations of these chemical groupings are most sensitive to environmental variations and undergo marked and characteristic changes as a result of them.

D_2O, possessing a relatively transparent spectroscopic window from 1300 to 1800 cm^{-1}, has permitted the development of a number of flexible spectroscopic methods for investigating polynucleotide interaction. Having found that reliable absolute intensity measurements can be made of D_2O solutions (Miles, 1958), we have developed quantitative computer methods based upon accurate intensity measurements (Miles & Frazier, 1964; Howard et al., 1966; Miles, 1971). With these analyses both qualitative identification of polynucleotide interaction products and quantitative determination of their amounts have been made in many cases (for review and discussion, see Miles, 1971). It is also possible to establish specificity of polynucleotide interactions by observing parallel temperature dependence of resolved bands assigned to the two components.

We have felt a need to apply such methods in H_2O in the 1650-cm^{-1} region in order to observe NH_2 deformations and the effect of coupling of NH and NH_2 bending modes on the carbonyl vibrations, and to aid in the interpretation of spectra observed in D_2O. Strong absorbance of water at ~1645 cm^{-1}, however, has previously prevented reliable measurement of infrared spectra in H_2O in the carbonyl region. By use of very short path length cells (5 μm) and computer subtraction of the water spectrum, we have obtained reliable spectra having resolved, clearly assignable bands of nucleotides and polynucleotides through the entire 1500–1800-cm^{-1} region. To avoid problems encountered with very thin cells, we have also employed mixed solvent methods, which reduce the concentration of H_2O and the absorbance of solvent, thus permitting use of longer path lengths and more convenient direct compensation double-beam spectroscopy. This method now makes the carbonyl region accessible in water as a solvent for the same kinds of experiments that have previously been possible only in D_2O.

Methods

Analysis of the difficulties presented by infrared spectroscopy in H_2O in the carbonyl region shows two ways of overcoming them. The central problem presented by water as an infrared solvent, its high absorbance, is due more to the low molecular weight and resulting high molar concentration of the solvent than to a high extinction coefficient. The concentration of water is 55.5 molar, and typical solute concentrations (e.g., 0.5–0.005 M) are more than 100-fold more dilute. The molar absorbance of water, however, is quite low: $\epsilon_{1645} = 18$ at 5 °C and $\epsilon_{1643} = 22$ at 70 °C (Figure 1). In contrast, the molar absorbance of the NH_2 deformation band of AMP is 600, or 30-fold greater than that of water (Figure 2). This AMP band, moreover, is much sharper than the broad HOH deformation band of water ($\Delta\nu_{1/2}$ 26 and 89 cm^{-1}, respectively at 5 °C).

The following equations and definitions are employed in spectroscopic methods described here:

$$\epsilon = A/ClE \qquad (1)$$

where ϵ is molar absorbance, A is observed net absorbance, C is concentration in moles per liter, l is path length in cm, and E is ordinate scale expansion factor. Units of ϵ are L mol^{-1} cm^{-1}.

$$A_{soln} - A_{solvent} = A_{solute} \qquad (2)$$

$$\epsilon_{H_2O} = A_{H_2O}/C_{H_2O}l \qquad (3)$$

$$\epsilon_{solute} = A_{soln}/C_{solute}l - A_{H_2O}/C_{H_2O}l \qquad (4)$$

[†] From the Laboratory of Molecular Biology, National Institute of Arthritis, Metabolism and Digestive Diseases, National Institutes of Health, Bethesda, Maryland 20014. *Received December 8, 1977.* A portion of this material was presented at the International Symposium on Biomolecular Structure, Conformation, Function and Evolution, Madras, India, January 4–7, 1978.

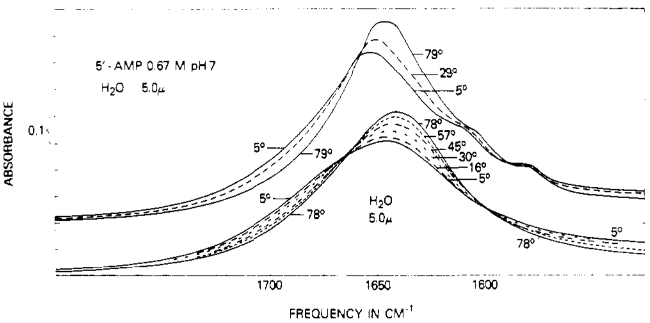

FIGURE 1: Infrared spectra of H_2O (lower curves) and of 5′-AMP (0.67 M) in H_2O (upper curves) in a 5.0 μm cell (CaF_2 windows, Teflon spacer). Uncompensated. Data were acquired directly by a computer, which subtracted solvent from solution spectra measured at the same temperature to produce the solute spectra in Figure 2. Molar absorbance of H_2O is 18 at 5 °C (1645 cm^{-1}) and 22 at 70 °C (1643 cm^{-1}).

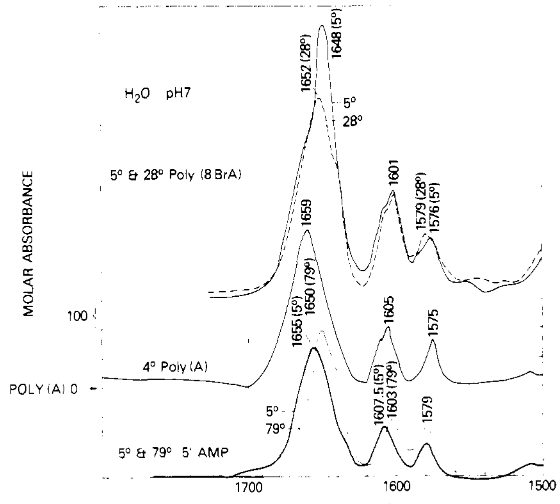

FIGURE 2: Infrared spectra in pure H_2O of 5′-AMP, poly(A), and poly(8BrA) obtained by computer subtraction of H_2O spectra (Figure 1) from solution spectra. The first two are on a molar absorbance scale for which index marks are 100 units apart. Poly(8BrA) is on an arbitrary scale, slightly more expanded than the lower two.

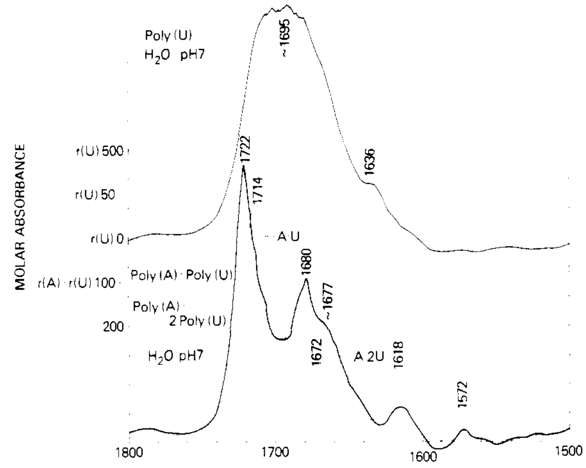

FIGURE 3: Infrared spectra in pure H_2O of random coil poly(U) (upper curve) and of the double (A•U) and triple (A•2U) helices formed with poly(A). Ordinate: molar absorbance. Index marks correspond to 50 units for rU and 100 units for rA•rU and rA•2rU.

C_{H_2O} is the molar concentration of water in water = 55.5 M. The net absorbance is obtained by subtracting observed values from the baseline value at a frequency taken to have zero absorbance (in these experiments, usually 1850 cm^{-1}).

Compensated spectra are obtained by computer subtraction of solvent spectra, measured previously in the same cell, from those of the solutions. The spectra are acquired by an on-line Honeywell 516 computer as uncorrected absorbance data measured at 0.5-cm^{-1} intervals. The subtraction, $A_{\text{soln}} - A_{\text{solvent}} = A_{\text{solute}}$, gives the solute spectrum, which is then normalized to a molar absorbance basis (eq 1). Since absorbance of H_2O increases linearly with temperature ($d\epsilon_{\max}/dT = 0.0625$; Figure 1), it is necessary to measure and subtract the solvent spectra at the same temperatures as the solutions.

We assembled short path cells (5–8 μm) from CaF_2 windows and spacers cut from Teflon tape of desired thickness (Dilectrix Corp.) Path length was determined by interference fringes. The relation between absorbance of H_2O at 1645 cm^{-1} (30 °C) and path length l in μm is given by $A = 0.107l$. For most solutes a path length of 7–8 μm is a practical upper limit for measurement in H_2O. High viscosity of the helical molecules made it difficult to avoid small air bubbles when filling 5-μm cells. The spectral quality was therefore often lower than that of nonviscous samples.

Reasons for adopting a solvent subtraction procedure in cases of very high solvent absorbance have been outlined previously (Miles, 1971). In the usual direct double-beam solvent compensation method, it is possible to encounter artifacts, due to stray light or unequal compensation, which may be difficult to recognize. It is therefore desirable to establish reliability of results by the subtraction method, even if subsequent experiments are carried out by the more convenient direct compensation method. There is, moreover, a major practical difficulty with the direct method at very short path length and high absorbance in that it requires almost perfectly matched cells. In practice we have not been able to achieve such a match at 6-μm path length. Using the same cell for solvent and solution, however, avoids this difficulty.

As we have noted above the main spectroscopic problem with water arises primarily from its high molar concentration. Our approach to improving the quality and usefulness of infrared spectra measured in water is therefore that of reducing the concentration of water, thus decreasing the magnitude of the second term in eq 4. This reduction in water concentration can be achieved by dilution with certain miscible organic solvents. We have found methanol, ethylene glycol, and dimethyl sulfoxide to be useful for this purpose. In using any diluent, it is first necessary to establish that the spectra are not significantly altered by the organic solvent. We observe in this study that spectra are essentially the same in the double-bond region in pure H_2O and in mixed solvents containing water (cf. Figures 2–8; for Figures 5 and 6, see paragraph concerning supplementary material at the end of this paper).

Confirmatory evidence of lack of spectroscopic perturbation by addition of relatively large amounts of organic solvent can be shown in D_2O solution. Here poly(G)•poly(C) was selected because of the large number of resolved bands in the double bond region. In Figure 9 we see that all seven vibrations of poly(G)•poly(C) in the double-bond region (for assignments and discussion of spectra, see Howard et al., 1969a; Miles, 1971) are virtually unchanged; in 60% Me_2SO, 40% D_2O, and even in 70% Me_2SO the only significant change is a loss of resolution of the cytosine ring vibrations at ~1624 and 1527 cm^{-1}. At lower concentrations of Me_2SO, the spectra are indistinguishable from those in D_2O.

We conclude that ribopolynucleotide infrared spectra in the

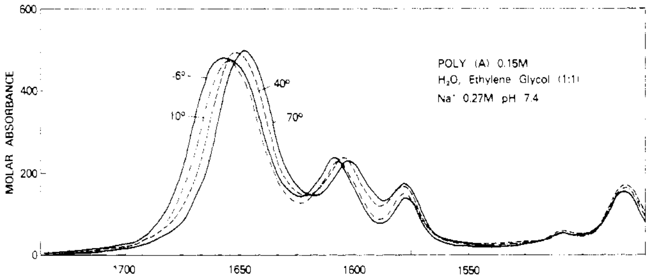

FIGURE 4: Infrared spectra of poly(A) in H_2O, ethylene glycol (1:1 by volume). Frequencies and intensities of bands are quite similar to those in pure H_2O (Figure 2).

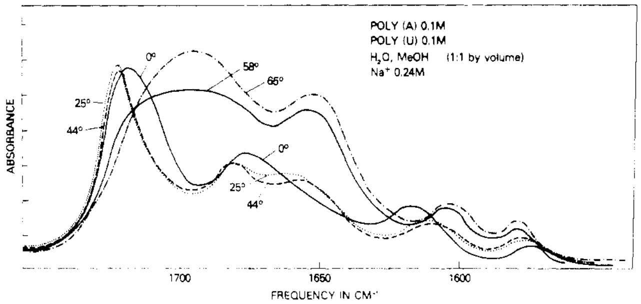

FIGURE 7: Infrared spectra of a 1:1 mixture of poly(A) and poly(U) in H_2O, methanol (1:1 by volume). The double helix present at 0 °C is converted to triple helix plus poly(A) at ambient temperature and to single-stranded forms at higher temperature. See text for discussion. Path length 12 μm. Scale expansion 5.71. Molar absorbance of the 1717-cm^{-1} A·U band at 0 °C is 387 (concentration 0.2 M) and that of the 1722-cm^{-1} A·U band at 44 °C is 525 (concentration 0.15 M).

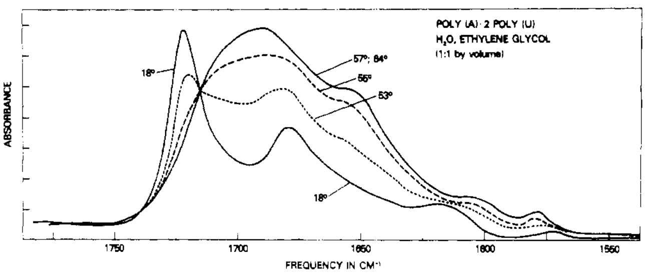

FIGURE 8: Infrared spectra of a 1:2 mixture of poly(A) and poly(U) as a function of temperature in H_2O, ethylene glycol (1:1 by volume). Compare 18 °C spectrum with that of triple helix in Figure 3.

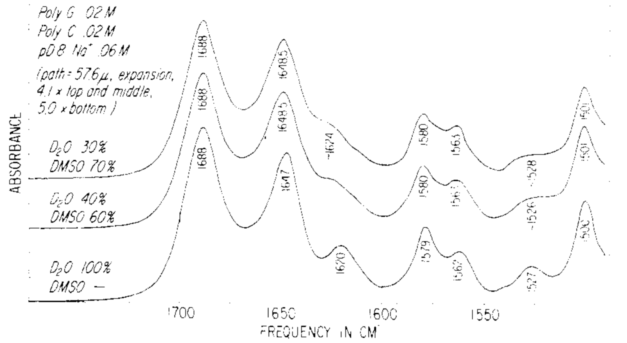

FIGURE 9: Infrared spectra of poly(G)·poly(C) in the double-bond region in pure D_2O (bottom) and in mixtures of D_2O and Me_2SO. As in H_2O, even large amounts of organic solvent have relatively small effects on the spectra, provided there is no change in secondary structure of the polymer.

carbonyl region are essentially the same in pure water or D_2O as in mixtures of water or of D_2O with methanol, ethylene glycol, or Me_2SO at the compositions employed here.

This conclusion is not surprising since the mixed solvents are still primarily aqueous. Thus, in 50 volume % methanol, for example, the molar concentration of methanol is 12.7 M and that of water is 28.8 M (Sober, 1966), corresponding to a mole fraction for H_2O of 0.694. The concentration of water is reduced and the usable path length correspondingly increased. If shorter or longer path lengths are desired, the molarity of water, C_{H_2O}, can be approximated by the relation C_{H_2O} = 0.569 (volume % methanol) and adjusted to the desired value. The need to match exactly the solvent composition of solution and reference is obvious.

The second point to consider with mixed solvents is the effect of organic solvents on polynucleotide secondary structure. In general, the same helix-coil transition occurs in the mixed aqueous solvents but with a lower T_m. With ethylene glycol, the decrease in T_m was found to be a nearly linear function of mole fraction of ethylene glycol, but even at $X_{glycol} = 0.60$ (volume fraction 82%) T_m of poly(I)·poly(C) is 30 °C and of poly(I)·poly(BrC) 58 °C (Howard et al., 1969b). A different kind of change in secondary structure of deoxypolynucleotides may occur at high concentrations of ethanol (60–80 volume %), in which DNA helices undergo a B → A conversion (Brahms & Mommaerts, 1964; Gray & Ratliff, 1975). In order to observe the B form of a deoxypolynucleotide helix, it would therefore be necessary to remain below the alcohol concentration at which this change occurs.

In the course of these experiments we have discovered a further effect of organic solvents on secondary structure. The conversion of double to triple A·2U helices is greatly facilitated by methanol or ethylene glycol, as is shown in a subsequent section. The effect of glycol on unstacking of single strands is also discussed below.

We have found that use of water diluted with organic solvents has major advantages, especially in observation of temperature dependence, though the ability to make measurements in pure H_2O remains important to verify results from mixed solvents. Mixtures of H_2O and organic solvents permit the use of longer path lengths. In our experience, assembly of 12-μm cells has proved much easier than 6-μm cells, and well-matched 12-μm pairs have been obtained. Spectra obtained by direct compensation with these cells are shown in Figures 4 and 6–8, and those obtained by computer subtraction with 6-μm cells are shown in Figures 2 and 3.

Results and Discussion

AMP and Poly(*A*). The spectra of AMP and poly(A) are closely similar, the latter having three bands at 1659, 1605, and 1575 cm^{-1} (Figure 2; values for poly(A), 4 °C). The band of AMP at 1579 cm^{-1} is the adenine ring vibration seen at the same frequency in D_2O, strong in Raman, relatively weak in the infrared. This intensity relationship is consistent with assignment to a mode having a major contribution from a stretching vibration of the C4–C5 double bond. We assign the strong band at 1659 cm^{-1}, which is absent in D_2O, to the NH_2 deformation. In the solid state strong infrared bands of adenine derivatives at about 1670 cm^{-1} have been assigned to δ_{NH_2} by a number of investigators (cf. Angell, 1961; Shimanouchi et al., 1964; Lord & Thomas, 1967). The band was considered by Shimanouchi et al. (1964) to be strongly coupled to a ring vibration and by Lord & Thomas (1967) to be a nearly pure scissoring motion. The higher frequency in the solid state is presumably due to more extensive hydrogen bonding than in solution. This band is too weak to be observed in the Raman (Lord & Thomas, 1967). The 1605-cm^{-1} band in H_2O is the analogue of the adenine ring vibration observed in D_2O at 1627 cm^{-1}, shifted to lower frequency by coupling to the NH_2 deformation. The uncoupled value of the ring vibration may be taken as that observed in D_2O (1627 cm^{-1}), and the "unperturbed" frequency of the NH_2 deformation may be close to this value (aniline, for example, has a value of 1620 cm^{-1}), favoring a strong coupling interaction. We have examined a related amino heterocycle for evidence of ring–NH_2 interaction and find that a qualitatively similar coupling appears to occur with 2-aminopyrimidine, though the frequencies, of course, are different. This compound in D_2O solution has ring vibrations at 1600 and 1568 cm^{-1}. In water the NH_2 deformation occurs at 1629 cm^{-1}, and the 1600-cm^{-1} (D_2O) ring vibration has been shifted down to ~1585 cm^{-1}, appearing as a shoulder on the side of a stronger ring vibration at 1573 cm^{-1}.

The two higher frequency bands of AMP show a similar temperature dependence between 5 and 80 °C. The NH_2 deformation has ν_{max} 1655 cm^{-1} at 5 °C, shifting progressively to 1650 cm^{-1} as the temperature is increased to 80 °C. The ring vibration at 1607.5 cm^{-1} decreases to 1603 cm^{-1} over the same range. We attribute the change of NH_2 frequency to decrease of hydrogen bonding to solvent on heating, and that of the ring vibration may be due either to its coupling to the NH_2 deformation, or to unstacking of the nucleotide, or to both. We note that there is also a monotonic decrease of frequency with temperature of the 1625-cm^{-1} ring vibration of AMP, 8BrADP, and poly(A) in D_2O, where NH_2 coupling cannot occur (Miles, 1971). It appears likely that stacking of the bases contributes to the shift of this band in D_2O.

Poly(A)·H_2O, Ethylene Glycol (50 Volume %). The spectrum (Figure 4) closely resembles that in pure H_2O (cf. Figure 2). δ_{NH_2} occurs at 1658 cm^{-1} at −5.6 °C and decreases linearly with temperature to 1648.5 cm^{-1} at 70 °C. The coupled ring vibration occurs at 1609 cm^{-1} at −5.6 °C, decreasing to 1602 at 70 °C. These maxima occur at slightly lower frequencies at a given temperature in the mixed solvent than in pure H_2O, presumably because of reduced stacking. The ring vibration at 1578 cm^{-1} changes only ~1 cm^{-1} over the same temperature range. Previous ORD and CD studies have shown that ethylene glycol causes destacking of such single stranded polymers as poly(A) and poly(C) (cf. Fasman et al., 1964; Green & Mahler, 1970; Lowe & Schellman, 1972, and references there cited). The above infrared results suggest that δ_{NH_2} is relatively insensitive to stacking, but a marked senstivity is observed in the antisymmetric PO_2^- stretching vibration in the 1240-cm^{-1} region. We describe these results because of their relevance to the A·U disproportionation reaction (see below), though they are outside the range primarily considered in this paper. The antisymmetric PO_2^- stretching vibration was originally assigned at 1220 cm^{-1} for dimethyl phosphate anion by Shimanouchi et al. (1964) and at ~1230 cm^{-1} in DNA films by Sutherland & Tsuboi (1957). In H_2O solutions of poly(A) we observe at 3 °C a strong band with a sharp maximum at 1243 cm^{-1} (ϵ 770) and unresolved absorption in the 1220–1230-cm^{-1} region (Figure 10). We assign the 1243-cm^{-1} band to the PO_2^- stretching vibration of a single backbone conformation or environment (as used here the latter term includes extent or nature of hydration), which predominates in poly(A) at low temperature. At 34 °C the 1243-cm^{-1} band has diminished in intensity, and a prominent shoulder is visible at ~1223 cm^{-1}. The 1243-cm^{-1} maximum disappears by 60 °C, and we observe a broad band with ν_{max} ≅ 1238 cm^{-1}. We attribute these changes observed on heating to creation of a broader distribution of conformations or environments and to depopulating the single conformation or environment (ν_{max} 1243 cm^{-1}) which is predominant at low temperature. (The bands discussed here are not due to adenine ring vibrations. In separate experiments we find that adenosine and 5′-AMP have very weak bands (ϵ < 100) in H_2O at 1254 and 1251 cm^{-1}, respectively, and an even weaker band at 1215 cm^{-1}. There are no other bands between 1200 and 1300 cm^{-1}.) The changes observed here, unlike those observed in CD or UV, do not arise directly from stacking, but since the processes of backbone conformational change and base stacking are evidently concomitant, the PO_2^- vibration can be used to monitor stacking. The effect of ethylene glycol on the spectrum is quite marked (Figure 10). Even at −5.5 °C there is only a broad band with ν_{max} ~ 1234 and ϵ_{max} 490, though in pure H_2O a strong resolved maximum persists at 34 °C (Figure 10). Heating the H_2O–glycol solution causes a reduction in ϵ_{max} and shift of the maximum of the band envelope to lower frequency as in the case of pure H_2O.

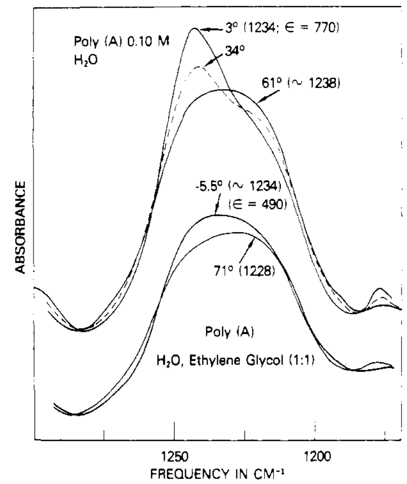

FIGURE 10: Antisymmetric PO_2^- stretching vibration of poly(A) in pure H_2O (top) and in H_2O, ethylene glycol (1:1) (bottom). At low temperature in pure H_2O a sharp maximum is observed at 1243 cm^{-1} (ϵ 770 at 3 °C) with a shoulder near 1220 cm^{-1}. At higher temperature the peak diminishes and the shoulder intensifies. We attribute the 1243-cm^{-1} peak to a single backbone conformation and environment about the phosphate which becomes progressively depopulated on heating. The destacking effect of glycol is seen in the lower spectra.

Poly(8BrA). The spectrum of poly(8BrA) in H_2O is quite similar to that of poly(A), but the bands occur at slightly lower frequencies. The 1648-cm^{-1} band (5 °C) is the NH_2 deformation, coupled to the ring vibration of 1601 cm^{-1}. An important structural conclusion can be drawn from this spectrum. In D_2O the ring vibration of the monomer 8BrADP occurs as a sharp band at 1627 cm^{-1}. The spectrum of poly(8BrA) in D_2O, however, is unique in that the ring vibration appears as a doublet with peaks of equal intensity at 1618.5 and 1633 cm^{-1} (Howard et al., 1974, 1975). The molecule exists as a double helix with BrA·BrA pairing, and the infrared doublet disappears as melting occurs to give a single band at the monomer value of 1627 cm^{-1}. In principle, three different explanations could account for this unprecedented doubling of the ring vibration, and these and their structural consequences have been discussed in a previous report (Howard et al., 1974). The explanation which is relevant to the present spectroscopic data is that identical BrA residues have different frequencies because they exist in different environments in the helix. This proposal would require a nonsymmetrical bonding scheme with one BrA residue bound at N7 and the other at N1. Equal population of the two environments would account for equal intensities of the two peaks. When the solvent is changed from D_2O to H_2O, the ring vibration shifts from a mean value of 1626 to 1601 cm^{-1} (Figure 2). The significant point for our

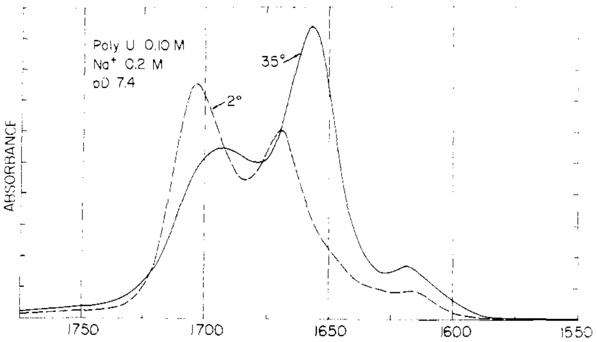

FIGURE 11: Spectra in D_2O of the helix (2 °C) and coil forms of poly(U). The highest frequency band (predominantly C_2 carbonyl) in the coil form intensifies and shifts to higher frequency on helix formation. The second band also increases in frequency but is reduced in intensity. For comparison, spectra in H_2O and H_2O, glycol (Figure 5 and 6 in supplementary material) show similar behavior of the resolved high frequency band, though with a larger frequency *shift*. The *second* carbonyl band is not resolved in H_2O but presumably accounts for absorbance on the low frequency side of the strong band of $\nu_{\max}$ 1706 cm^{-1}.

present purpose is that the ring vibration occurs as a single peak rather than an equal-intensity doublet with a peak separation of ~15 cm^{-1}. The NH_2 deformation also has a single strong peak. The vibrational spectra therefore provide no support for a nonsymmetrical structure having the paired BrA residues in different environments. We assume that Fermi resonance of a combination band with the fundamental ring vibration is the most probable explanation of the doublet. The conformational dependence of splitting would arise from a decrease in δ, the frequency separation of the interacting modes, when the helix is formed (for the original proposal and further discussion of conformation dependence of Fermi resonance in polynucleotides, see Ikeda et al., 1970; Miles, 1971). When the fundamental is shifted to 1601 cm^{-1} in H_2O, it is presumably too far removed from the postulated combination band for resonance to occur.

Recent CPF calculations on poly(8BrA) have indicated that of three possible BrA·BrA hydrogen bonding schemes only the symmetrical one mutually bonded at N_1 is capable of forming the basis of a regular helical structure (Govil et al., 1977). The present data are fully consistent with this conclusion.

Poly(U)·Pure H_2O. The spectrum of poly(U) has a strong, broad band at ~1695 cm^{-1} and a weak band at 1636 cm^{-1} (Figure 3). We expect three bands in the double bond region, and in D_2O solution these are observed at 1692, 1657, and 1618 cm^{-1} (cf. Figure 11). In the solid state normal NH derivatives of uracil also show three bands. We shall cite frequencies for the model compound 1-methyluracil, basing the assignments upon a study carried out by Lewis, Becker, & Miles (manuscript in preparation) with the aid of a number of isotopic derivatives (cf. Miles et al., 1973). The designations ν_4, ν_5, and ν_6 are used for the three vibrations observed in the region 1550-1800 cm^{-1}, listed in order of decreasing frequency. Polycrystalline 1MeU has ν_4 at 1695, ν_5 at 1660, and ν_6 at 1623 in the infrared. The maximum of the strong band observed in Figure 3 corresponds to that of ν_4, which has a major contribution from the C2 carbonyl stretching vibration. ν_5 occurs at 1660 cm^{-1} in solid 1MeU but is evidently not intense enough to appear as a resolved band in H_2O solution. The band envelope above 1650 cm^{-1} is too broad ($\Delta\nu_{1/2} \cong 60$ cm^{-1}) to be accounted for by a single carbonyl band, and skewing on the low frequency side suggests the presence of an unresolved band. In 1MeU ν_5 is unchanged by 2-^{18}O substitution but shifts to 1647 cm^{-1} on 4-^{18}O substitution (for uridine 4-^{18}O in D_2O, cf. Miles, 1964). These results indicate major C4 carbonyl stretching character of ν_5 in the 3NH species.

The poly(U) spectrum changes as the helix is formed upon cooling the solution (Figure 5, supplementary material) to give a peak with a sharp maximum at 1706 cm^{-1}, and a broad, skewed contour on the low frequency side. The 1695-cm^{-1} band in the coil is evidently perturbed by U·U interaction in the helix, showing an increase in frequency of 12 ± 1 cm^{-1} and in $A_{\max}$ of ~15%. ν_4 is still not resolved in the helix. Loss of intensity in the region below ~1690 cm^{-1} results in part from the shift of ν_4 but may also reflect a reduction in absorbance of ν_5, possibly with an accompanying frequency increase. ν_6 remains a weak shoulder at ~1635 cm^{-1}. For comparison we observe the helix → coil transition in D_2O solution (Figure 11). Here ν_4 also increases in frequency (to 1704 cm^{-1}) and intensity ($A_{\max}$), while ν_5 undergoes a frequency increase (from 1657 to 1670 cm^{-1}) and intensity decrease to produce the well resolved band observed at 2 °C (Figure 11). ν_6 undergoes slight decreases in frequency and intensity when the helix is formed. Lewis et al. found that ν_5 and ν_6 have quite different character in the two solvents as reflected by a different pattern of isotopic shifts, but ν_4 is similar in H_2O and D_2O.

The poly(U) helix evidently has a nonsymmetrical bonding scheme with antiparallel strands in which the C4 carbonyl in one strand is bonded by N3H and the C2 carbonyl in the other strand (Zimmerman, 1976; Thrierr et al., 1972).

Poly(U)·H_2O, Ethylene Glycol (50 Volume %). As in pure H_2O we observe at 30 °C a single broad band at ~1695 cm^{-1}, with unresolved absorption on the low frequency side of the band and a shoulder at ~1630 cm^{-1}. At −7 °C the helical form has $\nu_{\max}$ 1706 cm^{-1} and $\epsilon_{\max}$ 920 (values in pure H_2O for the helix, 1706 cm^{-1}, 950). There is an unresolved shoulder near 1670 cm^{-1} and a weak shoulder at ~1630 (Figure 6, supplementary material).

Poly(A)·Poly(U)·Pure H_2O. The spectrum of this two-stranded helix in H_2O has resolved bands at 1714, 1672, 1618, and 1572 cm^{-1} (Figure 3). The highest frequency band is assigned to the C_2 carbonyl vibration (ν_4) (for uridine assignments, see section on poly(U)), increased ~19 cm^{-1} from the monomer value by helix formation. The band with $\nu_{\max}$ 1672 cm^{-1} is assigned to the uridine C_4 carbonyl band (ν_5), the unresolved NH_2 deformation band of adenine presumably contributing to absorption on the low frequency side of the maximum. The band at 1618 cm^{-1} is the A ring vibration, shifted from the single strand (or monomer) value of 1605 cm^{-1}. The weak ring vibration at 1572 cm^{-1} has decreased slightly in frequency from the single strand value.

The large shift on A·U helix formation of ν_4 in H_2O solution contrasts with the lack of change in D_2O. 2-^{18}O isotopic labeling on 1-methyluracil (Miles et al., 1973) reveals that ν_4 is coupled to the N–H in-plane bending mode (amide II band at 1416 cm^{-1}) in H_2O, a relation which is abolished by solvent exchange in D_2O. Whether the frequency increase of ν_4 on A·U pair formation in H_2O is related to the increase of the amide II band ($\Delta\nu = 25$ cm^{-1}) is not clear.

In D_2O, ν_5 shifts from 1657 cm^{-1} to 1672 cm^{-1} (Miles & Frazier, 1964). The fact that there is also a band at 1672 cm^{-1} in H_2O is presumably fortuitous since the character of ν_5 in H_2O and D_2O is different, and the A–NH_2 bending vibration probably also occurs within the observed band envelope near this frequency. The larger shift of the A ring vibration in H_2O (~15 cm^{-1}) than in D_2O (~7 cm^{-1}) may be related to the effect of base pairing on coupling between this mode and δ_{NH_2} in water. The small decrease of the weaker ring vibration to ~1572 cm^{-1} is similar in both.

Poly(A)·2 Poly(U)·Pure H_2O. The spectrum of the triple helix has resolved bands at 1722, 1680, 1618, and 1572 cm^{-1}. We assign the first of these to the uridine C_2 carbonyl band, shifted ~27 cm^{-1} from the random coil (or monomer) value. The band at 1680 is assigned to ν_5 of U, and absorbance on the low frequency side of this band may be due to δ_{NH_2} of A. Hydrogen bonding would favor a high frequency for δ_{NH_2}, and in the solid state this vibration occurs at ~1670 cm^{-1}. The bands at 1618 and 1572 cm^{-1} are assigned to the two adenine ring vibrations, as in the case of poly(A)·poly(U).

Poly(A)·Poly(U)·H_2O, Methanol (50 Volume %). The quality of spectra measured in this mixed solvent (mole fraction H_2O, 0.694; molar concentration H_2O, 28.8) (Figure 7) is much higher than that in pure water, for reasons noted above, and the experimental convenience of temperature variation is much greater. Since we observe quite similar spectra in the two solvents, it appears that the specifically spectroscopic effects of introducing 50% methanol are small. In this case, however, we must deal with the chemical consequences of adding an organic solvent to water.

The spectrum observed at 25 °C (Figure 7) resembles not that of the double helix in H_2O but that of the triple helix (Figures 3 and 8), with an additional band at 1659 cm^{-1} corresponding to the NH_2 bending vibration of single-stranded poly(A). This pattern suggested the occurrence below ambient temperature of strand disproportionation, a reaction which was first discovered by infrared spectroscopy in D_2O solution (Miles & Frazier, 1964):

$$2A{\cdot}U \rightarrow A{\cdot}2U + A$$

In pure D_2O or H_2O, however, the reaction had a 2 → 3 transition temperature of 45 °C in Na^+ 0.14 M, Mg^{2+} 0.01 M. Cooling the H_2O, MeOH solution results in spectral changes observed in Figure 7. The carbonyl band shifts from 1722 to 1717 cm^{-1} at 0 °C, the resolved A δ_{NH_2} band at 1659 cm^{-1} disappears, and the A ring vibration shifts from 1608 to 1618 cm^{-1}. These changes correspond to those expected for reversal of the disproportionation reaction, and the frequencies are those observed for A·U in pure H_2O, except that the carbonyl frequencies are 3 cm^{-1} higher in the mixed solvent. Infrared temperature profiles measured at frequencies assignable to specific vibrations in A and U are shown in Figure 12. There are two phase transitions, one with T_m = 20 °C and a second with T_m = 56 °C. The fact that resolved bands of U (1696, 1710 cm^{-1}) and A (1654, 1603) exhibit a parallel temperature dependence shows that the spectral changes result from specific A·U base pairing association (for more detailed discussion of this point cf. Howard et al., 1969; Miles, 1971). Frequencies of the bands observed in the plateau spectra (25–50 °C) and after melting of the helices (60 °C) show that the two transitions of T_m 20 and 56 °C correspond, respectively, to the following reactions:

$$2A{\cdot}U \rightarrow A{\cdot}2U + A$$

$$A{\cdot}2U \rightarrow A + 2U$$

Further confirmation of the nature of these transitions is obtained by analysis of the spectra in Figure 7 by a computer method developed previously for D_2O solutions (cf. Miles & Frazier, 1964; Howard et al., 1966; Miles, 1971). Analysed in terms of A, U, and AU_2 the plateau spectrum in Figure 7 shows 78% AU_2, 19% A, and 3% U, compared with the expected values of 75, 25, and 0% (the small error appears to be due to an incorrect ratio of A and U in the basis spectrum for AU_2). At 58 °C the analysis shows 51% A and 48% U. T_m of the 3 → 1 transition is slightly lower than in pure H_2O at this salt concentration as a result of depression by the organic solvent. For ethylene glycol this depression was observed to be essentially linear for poly(I)·poly(C) and poly(I)·poly(BrC) when expressed as mole fraction of organic solvent, but was quite nonlinear when expressed as volume fraction. Fifty volume percent organic solvent produced a relatively small depression of T_m (Howard et al., 1969). The large reduction of $T_{2\rightarrow3}$ ($\Delta T_m \cong$ 38 °C) must be due to other factors, and we conclude that it is probably caused by unstacking of single-stranded poly(A) by the organic solvent. Ross & Scruggs (1965) pointed out that, since the disproportionation has a positive enthalpy, the reaction must be entropically driven. The entropy increase is presumably related to the greater conformational freedom of poly(A) in the single-stranded form. This freedom would be further increased by unstacking of poly(A), caused by the organic solvent (cf. section on poly(A)), and we propose that it is this effect of the methanol that is responsible for the large reduction of $T_{2\rightarrow3}$. We have carried out the same experiment in 50% H_2O, ethylene glycol and find the same result, indicating that the effect is not specific to methanol.

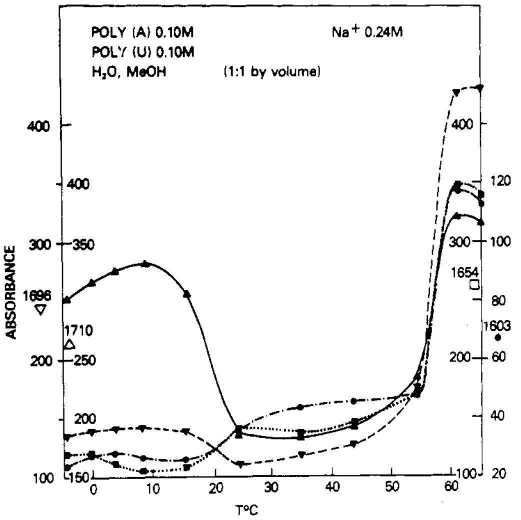

FIGURE 12: Infrared temperature profiles of 1:1 poly(A), poly(U) mixture (Figure 7). The first transition (T_m 20 °C) is a 2 → 3 disproportionation reaction (see text) and the second (T_m 56 °C) conversion of the triple helix to single strands. The organic solvent is responsible for a much lower T_m for the first transition than that in H_2O.

Poly(A)·2 Poly(U)·H_2O, Ethylene Glycol (50 Volume %). The spectrum of the triple helix (Figure 8) has resolved bands at 1722, 1679.5, 1618, and 1572 cm^{-1}. The values in pure H_2O are 1722, 1680, 1618, and 1572 cm^{-1} (Figure 3). There is also unresolved absorption near 1675 cm^{-1}. The first two bands are uridine carbonyl vibrations and the last two adenine ring vibrations, as discussed in a previous section. The spectra change progressively as the helix is melted, reaching at 60 °C a spectrum which is identical with a summation of the two components at 60 °C. An isosbestic point is observed at 1715 cm^{-1}, indicating that only two species are present during the transition (cf. Howard et al., 1969; Miles, 1971). Infrared temperature profiles (Figure 13; paragraph concerning supplementary material at the end of this paper) show a single-step melting curve with T_m = 54 °C for the 3 → 1 transition.

$2NH_26NMeA$·Poly(U): Helix Formed between a Nucleoside and Poly(U)·H_2O, Ethylene Glycol (1:1). Formation of helical complexes between purine monomers and pyrimidine polynucleotides was discovered by infrared spectroscopy in D_2O solution (Howard et al., 1964) and has been extensively studied by this method (Howard et al., 1966, 1969a; Ikeda et al., 1970; Hattori et al., 1976). The complex formed by 2-amino-6-*N*-methyladenosine with poly(U) is a double helix

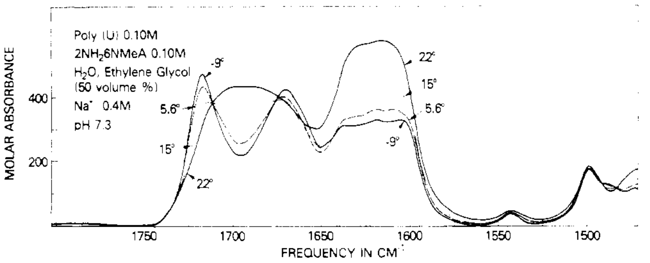

FIGURE 14: Infrared spectra of monomer–polymer helix formed by 2-amino-6-*N*-methyladenosine and poly(U) (−9 °C; H_2O, ethylene glycol 1:1). This Watson–Crick helix has U carbonyl maxima at the same frequencies (1717, 1672 cm^{-1}) as poly(A)·poly(U) (Figure 3). The isosbestic point at 1709 cm^{-1} in the region of uridine absorbance indicates that U residues are present in only two environments during melting.

with Watson–Crick hydrogen bonding since the NMe group blocks attachment of a third strand, and the $2\text{-}NH_2$ group causes the same elevation of T_m observed with 2-aminoadenosine (Ikeda et al., 1970; cf. Howard et al., 1966). We shall first use the new data to show that a specifically hydrogen bonded complex is formed under these conditions (50% glycol) and later discuss explicitly the spectrum of the complex (Figure 14). The temperature profiles of bands assignable exclusively to U (1717, 1690 cm^{-1}) or to A (1614 cm^{-1}) vibrations exhibit parallel melting behavior (Figure 15), showing that the spectroscopic changes result from specific A·U interation rather than from self-structures of either component (cf. Miles & Frazier, 1964; Miles, 1971). In the present case the monomeric component forms no independent self-structure, and poly(U) forms one with a different spectrum and lower stability. The set of infrared spectra (Figure 14) generated by heating the solution has an isosbestic point at 1709 cm^{-1} (where only U absorbs), indicating that poly(U) occurs in only two environments during melting: A·U helix and random coil. A computer analysis of the spectrum at 14.9 °C (slightly above T_m) was carried out in terms of spectra of the two components and of the mixture at the lowest observed temperature (the extent of interaction at −9 °C is evidently greater than 90% and may be ~95%). The analysis indicated 29% monomer, 31% poly(U), and 40% complex (−9 °C spectrum), in satisfactory agreement with the fraction melted expected from the temperature profiles. We note that the T_m in this solvent is ~17 °C lower than in pure D_2O at about the same salt and monomer concentration (Ikeda et al., 1970) and attribute the difference to the destabilizing effect of glycol.

The infrared spectrum of this monomer–polymer helix in D_2O is unusual in having three strong bands (1699, 1669, 1648 cm^{-1}) in a region where poly(A)·poly(U) (1691, 1672 cm^{-1}) or poly($2NH_2 6NMeA$)·poly(U) (1689, 1668 cm^{-1}) have only two (Ikeda et al., 1970). Conformation-dependent Fermi resonance has been proposed to account for the band at 1648 cm^{-1}, which is not present in the polymer–polymer helix (Ikeda et al., 1970). The infrared spectrum of the same complex in H_2O, ethylene glycol (1:1; mol fraction H_2O ~0.76; −9 °C) is shown in Figure 14. Here the anomaly seen in D_2O is not observed, though there is an additional band in the lower frequency region. There are two strong bands at the same frequencies as those of poly(A)·poly(U) (1717, 1670 cm^{-1}) and no others above 1640 cm^{-1}. The spectrum is in fact simpler than that of the A·U helix. There is no unresolved absorption on the low frequency side of the 1670 cm^{-1} peak caused by the $A\text{-}NH_2$ bending vibration (cf. Figures 3 and 7), which is absent because of NMe substitution.

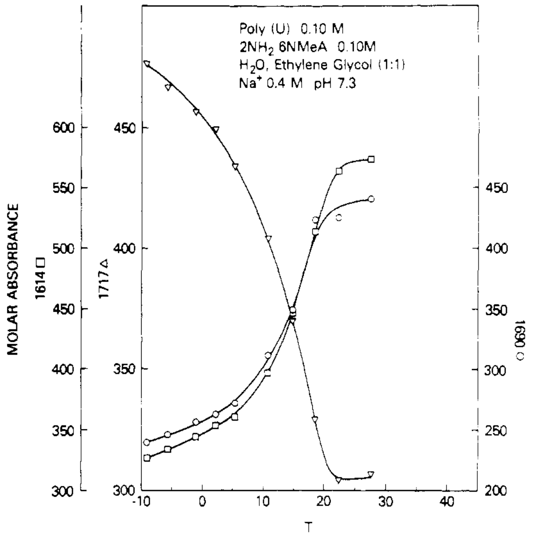

FIGURE 15: Infrared melting curves of monomer–polymer helix from spectra of Figure 14. Parallel temperature dependence of resolved A (1614 cm^{-1}) and U (1717, 1690 cm^{-1}) bands shows that the spectral changes observed in Figure 14 result from specific A·U interaction (cf. text).

Between 1600 and 1650 cm^{-1} are three bands, not well resolved, at ~1638, 1619, and 1604 cm^{-1}. The free monomer has two A ring vibrations in this region: a strong shoulder at ~1630 cm^{-1} and a peak at 1618 cm^{-1} (−2 °C). The first does not change significantly with temperature but the second shifts to 1609 cm^{-1} by 50 °C, with no change of intensity.

Supplementary Material Available

Figures 5, 6, and 13 (3 pages). Ordering information is given on any current masthead page.

References

Angell, C. L. (1961) *J. Chem. Soc.*, 504–515.

Brahms, J., & Mommaerts, W. H. F. M. (1964) *J. Mol. Biol. 10*, 73–88.

Cotter, R. I., & Gratzer, W. B. (1969) *Nature (London) 221*, 154–158.

Fasman, G. D., Lindblow, C., & Grossman, L. (1964) *Biochemistry 3*, 1015–1020.

Govil, G., Fisk, C., Howard, F. B., & Miles, H. T. (1977) *Nucleic Acids Res. 4*, 2573–2592.

Gray, D. M., & Ratliff, F. L. (1975) *Biopolymers 14*, 487–498.

Green, G., & Mahler, H. R. (1970) *Biochemistry 9*, 368–387.

Hattori, M., Frazier, J., & Miles, H. T. (1975) *Biochemistry 14*, 5033–5045.

Hattori, M., Frazier, J., & Miles, H. T. (1976) *Biopolymers 15*, 523–531.

Howard, F. B., Frazier, J., Lipsett, M. N., & Miles, H. T. (1964) *Biochem. Biophys. Res. Commun. 17*, 93–102.

Howard, F. B., Frazier, J., Singer, M. F., & Miles, H. T. (1966) *J. Mol. Biol. 16*, 415–439.

Howard, F. B., Frazier, J., & Miles, H. T. (1969a) *Proc. Natl. Acad. Sci. U.S.A. 64*, 451–458.

Howard, F. B., Frazier, J., & Miles, H. T. (1969b) *J. Biol. Chem. 244*, 1291–1302.

Howard, F. B., Frazier, J., & Miles, H. T. (1971) *J. Biol. Chem. 246*, 7073–7086.

Howard, F. B., Miles, H. T., & Frazier, J. (1974) *J. Biol. Chem. 249*, 2987–2990.

Howard, F. B., Frazier, J., & Miles, H. T. (1975) *J. Biol.*

Chem. 250, 3951-3959.
Howard, F. B., Frazier, J., & Miles, H. T. (1976) *Biochemistry 15*, 3783-3795.
Ikeda, K., Frazier, J., & Miles, H. T. (1970) *J. Mol. Biol. 54*, 59-84.
Lord, R. C., & Thomas, G. J., Jr. (1967) *Spectrochim. Acta 23A*, 2551-2591.
Lowe, M. J., & Schellman, J. A. (1972) *J. Mol. Biol. 65*, 91-109.
Miles, H. T. (1958) *Biochim. Biophys. Acta 30*, 324-328.
Miles, H. T. (1964) *Proc. Natl. Acad. Sci. U.S.A. 51*, 1104-1109.
Miles, H. T. (1971) *Proced. Nucleic Acid Res. 2*, 205-232.
Miles, H. T., & Frazier, J. (1964) *Biochem. Biophys. Res. Commun. 14*, 21-28.
Miles, H. T., Lewis, T. P., Becker, E. D., & Frazier, J. (1973) *J. Biol. Chem. 248*, 1115-1117.
Morikawa, K., Tsuboi, M., Takabashi, S., Kyogoku, Y., Mitsui, Y., Iitaka, Y., & Thomas, G. J., Jr. (1973) *Biopolymers 12*, 799-816.
Ross, P. D., & Scruggs, R. L. (1965) *Biopolymers 3*, 491-496.
Shimanouchi, T., Tsuboi, M., & Kyogoku, Y. (1964) *Adv. Chem. Phys. 7*, 435-498.
Sober, H. A., Ed. (1966) *Handbook of Chemistry and Physics*, p D157, Chemical Rubber Publishing Co., Cleveland, Ohio.
Sutherland, G. B. B. M., & Tsuboi, M. (1957) *Proc. R. Soc. London, Ser. A 239*, 446-463.
Thomas, G. J., Jr. (1969) *Biopolymers 7*, 325-334.
Thrierr, J. C., Deubel, V., & Leng, M. (1972) *Biochimie 58*, 1115-1119.
Tsubor, M. (1969) *Appl. Spectrosc. Rev. 3*, 45-90.
Zimmerman, S. B. (1976) *J. Mol. Biol. 101*, 563-565.

Coat Protein Binds to the 3′-Terminal Part of RNA 4 of Alfalfa Mosaic Virus[†]

Corrie J. Houwing and E. M. J. Jaspars*

ABSTRACT: All four RNAs of alfalfa mosaic virus contain a limited number of sites with a high affinity for coat protein [Van Boxsel, J. A. M. (1976), Ph.D. Thesis, University of Leiden]. In order to localize these sites in the viral RNAs, RNA 4 (the subgenomic messenger for coat protein) was subjected to a very mild digestion with ribonuclease T1. The ten major fragments, apparently resulting from five preferential hits, were separated and tested for messenger activity in a wheat germ cell-free system, as well as for the capacity to withdraw coat protein from intact particles. Fragments which stimulated amino acid incorporation were assumed to contain the 5′ terminus. Strong evidence was obtained for the location of sites with a high affinity for coat protein near the 3′ terminus. The smallest fragment which has the 3′-terminal cytosine comprises only 10% of the length of intact RNA 4 but still possesses these sites. Evidence is presented that the complete coat protein cistron is in the complementing 90% fragment. Possibly, the high-affinity sites are entirely located in the 3′-terminal extracistronic part of RNA 4. They will have the same position in RNA 3 and, possibly, also in the other parts of the genome of alfalfa mosaic virus. The need of this genome for coat protein in order to become infectious may therefore find its explanation in the fact that a conformational change at the 3′ ends of the genome parts brought about by the coat protein is required for recognition by the viral replicase.

Alfalfa mosaic virus belongs to the group of plant viruses with a tripartite RNA genome. These viruses either have their genome parts (referred to as RNAs 1, 2, and 3) in separate virions of identical size (isocapsidic viruses) or of different size (heterocapsidic viruses). The heterocapsidic viruses share a unique biological property: they need a small amount of coat protein to start an infection cycle. Either coat protein itself or coat protein messenger from the same virus or from another heterocapsidic virus must be present to make the genome RNAs infectious. The coat protein messenger, referred to as RNA 4, is a small subgenomic RNA homologous to a part of RNA 3 (see Van Vloten-Doting and Jaspars, 1977, for a review). With the heterocapsidic AMV,[1] RNA 4 is mainly found in two copies in a special class of particles, the so called top component *a*. RNA 4 of AMV strain 425 has a length of about 800 nucleotides (Heijtink et al., 1977), of which 663 represent the cistron for the coat protein (Van Beynum et al., 1977; Koper-Zwarthoff et al., 1977).

The early function of the coat protein of the heterocapsidic viruses, though discovered in 1971 (Bol et al., 1971), is still a puzzling phenomenon. Apparently, the protein is needed in vivo, directly or indirectly, for an adequate expression of the coat protein cistron on RNA 3. If not, an infection with the three genome RNAs would start autonomously. However, no significant effect of the coat protein on the translation of AMV RNAs has been found in the cell-free systems from wheat germ (Van Vloten-Doting et al., 1975; Thang et al., 1975; Gerlinger et al., 1977; Rutgers, 1977) and Krebs ascites cells (Mohier et al., 1976), nor in oocytes of *Xenopus* (Rutgers, 1977).

Recent work from our group has shown that there are a few sites on the RNA molecules of AMV where coat protein sub-

---

[†] From the Department of Biochemistry, State University, Leiden, The Netherlands. *Received January 10, 1978*. This work was sponsored in part by the Netherlands Foundation for Chemical Research (S.O.N.), with financial aid from the Netherlands Organization for the Advancement of Pure Research (Z.W.O.).

[1] Abbreviations used: AMV, alfalfa mosaic virus; EDTA, ethylenediaminetetraacetate; TYMV, turnip yellow mosaic virus; tRNA, transfer RNA.

0006-2960/78/0417-2927$01.00/0